

Short-Range Order in KPO_3 Glass Studied by Neutron and X-Ray Diffraction

Uwe Hoppe^a, Günter Walter^a, Dörte Stachel^b, and Alex C. Hannon^c

^a Rostock University, Department of Physics, D-18051 Rostock

^b Friedrich Schiller University Jena, Otto Schott Institute, Faculty of Chemistry and Earth Sciences, D-07743 Jena

^c ISIS Facility, Rutherford Appleton Laboratory, Chilton, Didcot, OX11 0QX, UK

Z. Naturforsch. **51a**, 179–186 (1996); received January 27, 1996

The short-range order of KPO_3 glass has been studied by diffraction methods in order to make evident the different behaviour of the P-O bonds within the PO_4 tetrahedron. The oxygen sites are divided into bridging and terminal (non-bridging) oxygen sites, corresponding to two P-O bond lengths, the difference of which amounts to 14.5 pm. Previous conclusions about the changes of the P-O bond lengths under the influence of modifier cations of different electric field strength are corroborated. The K-O environments reveal two apparently different distances r_{KO} with equal contributions to the total K-O coordination number of about 6.7. To explain this phenomenon, the K^+ cations are suggested to be located in non-spherical cavities.

Key words: Neutron diffraction, X-ray diffraction, Phosphate glasses, Short-range order, Reverse Monte Carlo simulation.

1. Introduction

Because of its extrem position in systems with metaphosphate composition, KPO_3 glass was chosen for structural investigations by neutron and X-ray diffraction. KPO_3 glass is the chain phosphate containing the modifier ion of the lowest electric field strength, which can still be prepared in the vitreous state.

Neutron diffraction studies performed with spallation sources provide measurements up to high magnitudes of momentum transfer with $Q_{\text{max}} > 400 \text{ nm}^{-1}$, which offer an excellent real-space resolution. Results of such experiments on several binary metaphosphate glasses with modifier cations Na^+ [1]; Al^{3+} , Mg^{2+} , Zn^{2+} , and Pb^{2+} [2] reveal 2 different P-O bond lengths existing in the PO_4 tetrahedron. The frequencies of both P-O bonds were found to be equal. Since in glasses of metaphosphate composition the PO_4 units are linked by 2 of their 4 vertices with neighbouring tetrahedra, the unlike distances can be related to the bridging and the terminal (or non-bridging) oxygen sites, respectively.

Modifier cations of high electric field strength reduce the difference between the P-O bond lengths [2]. This phenomenon was attributed to changes of two P-O bond lengths in opposite direction. The deforma-

tion of the electron population in the molecular structures of the anionic PO_4 units caused by the electric field of adjacent modifier cations has consequences for the P-O bond lengths. This gives a qualitative explanation which can be understood in terms of an intermolecular interaction in the donor-acceptor approach [3]. Recently published results of ab initio molecular orbital (MO) calculations on the electronic structure of a series of clusters from pairs of linked PO_4 middle groups surrounded by various alkali ions led to similar conclusions [4]. Thus, the large K^+ cation with its small charge is excellently suited in order to examine the correlations of charge transfer and bond length changes.

A further point of interest concerns the coordination sphere of the potassium cation. The modifier ions are preferably surrounded by the terminal oxygen atoms (NBO). In metaphosphate glasses the number of NBO atoms per alkali modifier cation is equal to 2. Hence, large modifier cations forming extended coordination polyhedra must compete for the oxygen atoms in their coordination sphere. A broadening of the metal-oxygen (Me-O) distance peak, which could be almost called a splitting, was observed in a sodium disilicate glass [5], a system containing only one NBO atom per alkali ion. This effect was not detected in the NaPO_3 glass with 2 NBO atoms per Na^+ [5]. Therefore, the deficit of NBO atoms was suggested to be responsible for the broad Na-O peak obtained in the

Reprint requests to Dr. U. Hoppe, Fax 0381 498 17 26.

0932-0784 / 96 / 0300-0179 \$ 06.00 © – Verlag der Zeitschrift für Naturforschung, D-72072 Tübingen



Dieses Werk wurde im Jahr 2013 vom Verlag Zeitschrift für Naturforschung in Zusammenarbeit mit der Max-Planck-Gesellschaft zur Förderung der Wissenschaften e.V. digitalisiert und unter folgender Lizenz veröffentlicht: Creative Commons Namensnennung-Keine Bearbeitung 3.0 Deutschland Lizenz.

Zum 01.01.2015 ist eine Anpassung der Lizenzbedingungen (Entfall der Creative Commons Lizenzbedingung „Keine Bearbeitung“) beabsichtigt, um eine Nachnutzung auch im Rahmen zukünftiger wissenschaftlicher Nutzungsformen zu ermöglichen.

This work has been digitalized and published in 2013 by Verlag Zeitschrift für Naturforschung in cooperation with the Max Planck Society for the Advancement of Science under a Creative Commons Attribution-NoDerivs 3.0 Germany License.

On 01.01.2015 it is planned to change the License Conditions (the removal of the Creative Commons License condition “no derivative works”). This is to allow reuse in the area of future scientific usage.

disilicate system. For the K^+ cation, being significantly larger than the Na^+ cation, a similar broadening (or splitting) of the Me-O peak is even expected to be formed in the metaphosphate glass.

From a first view on the structure of a KPO_3 crystal [6] a rough estimation of the K-O bond length can be made ($r_{\text{KO}} \cong 0.28$ nm). As to the large K-O distance, the corresponding peak should be located in the vicinity of several other pair distances in the total $T(r)$ function. For this reason a reliable determination of the K-O coordination number, N_{KO} , from the results of a single diffraction experiment is difficult. The contrast of neutron and X-ray diffraction curves offers a chance to determine the parameters of the K-O sphere. In addition Reverse Monte Carlo simulations were used as a tool for extracting structural information in a range of distances larger than bond lengths. A comprehensive analysis of the concerning results will be given in a separate paper. Here only the partial correlation functions of a model configuration will be presented.

2. Experimental

2.1 Sample preparation

The raw material of the glass was powdered and dried KPO_3 (Piesteritz). The melt was held for 30 minutes at 900°C in a silica crucible (Heinersdorf). In order to obtain vitreous KPO_3 , drops of the melt were pressed between water cooled blocks of copper. In order to prevent moisture attack, the slab-shaped pieces of glass produced this way were preserved in CCl_4 . Just before the measurement, after drying, the pieces were crushed into a grain-shaped powder. Opal areas of the material, obviously enriched by crystallites, were kept away from the sample. For measurement of the mass density by Archimedes method and for the compositional analysis by an electron microprobe X-ray analyzer, clear pieces of the material were used as well. The mass density and the content of modifier oxide K_2O were found to be 2.416 g cm^{-3} and 49.3 mol%, respectively.

2.2 Diffraction experiments

The neutron diffraction experiment was performed using the time-of-flight technique on the "liquids and amorphous diffractometer" (LAD) at the neutron spallation source ISIS of the Rutherford Appleton

Laboratory, Chilton, England. The grain shaped glass sample was filled into a thin-walled vanadium container of 11 mm in diameter. A minor component of a scattering contribution from small crystallites was detected in the resulting differential cross-sections. The small Bragg reflexions were cleared away from the final neutron scattering curves. The data from all of the 14 detectors positioned at scattering angles 2θ between 5° and 150° were corrected by standard procedures for attenuation, multiple scattering, inelasticity effects, and for container and background scattering [7].

For the X-ray diffraction experiment, a grain shaped glass sample was used as well, which was filled into a capillary made from silica with 1 mm inner diameter. The measurement was performed in a step scan mode on a horizontal goniometer using Ag K_α radiation with scattering angles 2θ from 3° to 130° . The correction procedures which finally yield the normalized intensities were described in [8].

3. Results

The total structure factors, $S(Q)$, were calculated from the experimental intensities in the notation according to Faber and Ziman [9], which is extensively described in the textbook of Waseda [10]. Both $S(Q)$ functions, extracted from neutron and X-ray diffraction, are shown in Figure 1. Q is the magnitude of momentum transfer for the elastic scattering, with $Q = 4\pi/\lambda \sin \theta$, and λ is the wavelength of the radiation. The high- Q range of the neutron scattering curve is included in a separate plot (Figure 3).

The Fourier transforms of $S(Q)$ curves, the total distance correlation functions, $T(r)$, are shown in Figs. 2a, b, where the upper termination limits, Q_{max} , in the integrals were chosen to be 420 nm^{-1} and 202 nm^{-1} for the neutron and X-ray results, respectively. For details of the transformation procedure compare [2, 8]. No modification of the integrand by a damping factor was applied.

The methods for extracting the short-range order parameters from the $T(r)$ curves by least-squares fitting techniques applied with the termination effect taken into account are described in [8, 11]. The corresponding parameters for the distance peaks as Gaussian curves are given in Table 1. The model curves from a fit simultaneously performed to the experimental neutron and X-ray $T(r)$ functions are shown in

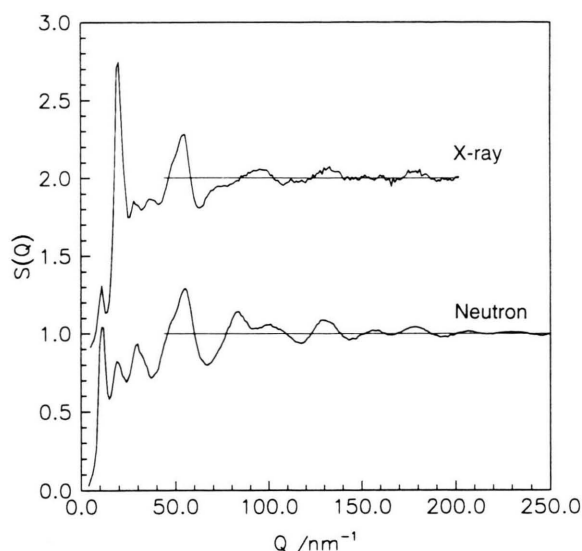
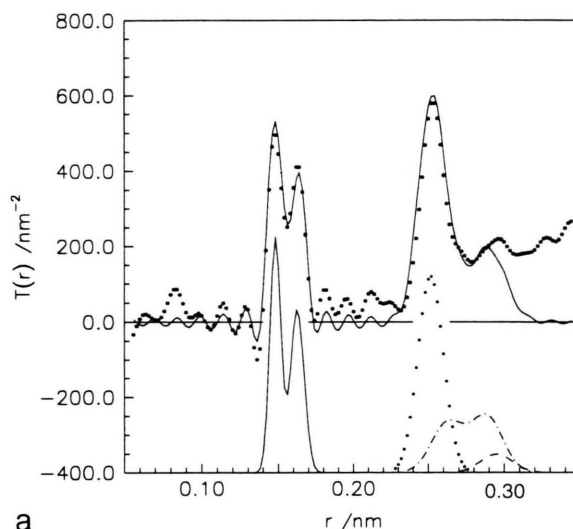


Fig. 1. Experimental total structure factors of the KPO_3 glass studied; The X-ray scattering curve is shifted by 1 for clearness of the plot. The high- Q range of the neutron scattering curve is included in Figure 3.

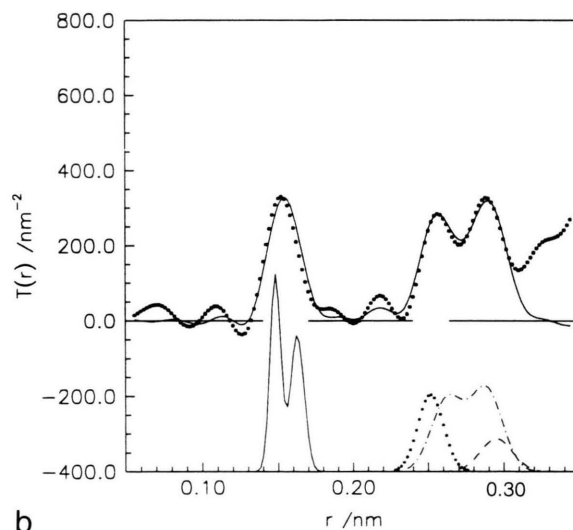
Figures 2a, b. The respective pair contributions are given in their original, unbroadened shape in the lower part of the plots.

First of all, the P-O distance peak at 0.155 nm was evaluated, where the high real-space resolution of the neutron result with the peak markedly splitted into two components (Fig. 2a) was the decisive issue. The difference of both P-O bond lengths turned out to be 14.5 pm. Two Gaussian curves were used for the approximation of the shape of the bond length distribution.

In order to demonstrate the contribution of the splitted peak to the scattered intensity, a backtransformation of the P-O model peak was performed. The final curve is shown in Fig. 3 and compared with the experimental result in terms of the weighted interference function $Q i(Q)$, with $i(Q) = S(Q) - 1$. Obviously, the high- Q range of the curve is dominated by interferences merely caused from the P-O bond lengths which possess the most narrow distance distributions with the smallest full widths at half maximum (fwhm) (see Table 1). The $Q i(Q)$ function (Fig. 3) shows a short and a considerably longer period of oscillations, which is a typical behaviour for two peaks from distances being not much different from each other. The shorter of the periods can be related to the mean P-O bond length. This period is about 12.3 times repeated



a



b

Fig. 2a, b. Total distance correlation functions calculated from the curves shown in Fig. 1 (dots) compared with the fitted curves (solid line). On the top (a): neutron scattering, at bottom (b): X-ray scattering. In the lower part of the plots, shifted for clearness, the pair peaks are given in their original shape; P-O solid line, O-O dots, Me-O dash-dotted line, P-P dashed line.

in the full range up to 500 nm^{-1} , which yields a mean bond distance of 0.154 nm. Note, half of a period was added taking into account the phase shift attributable to a change of the sign of the beat amplitude at about 220 nm^{-1} . The length of the range up to 220 nm^{-1} can be assigned to the half of the beat cycle. This value

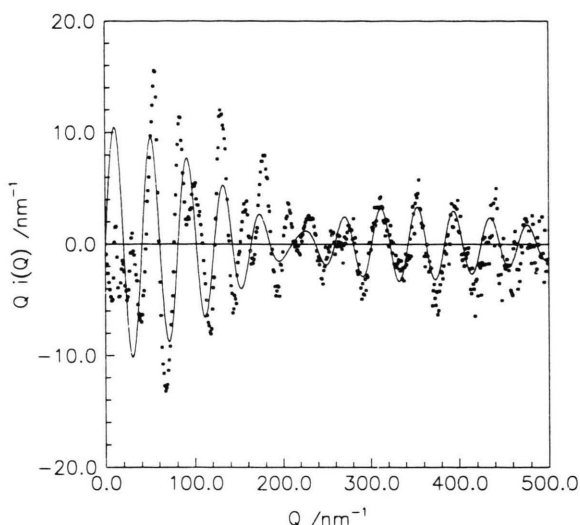


Fig. 3. Weighted interference function $Q i(Q)$, with $i(Q) = S(Q) - 1$, extracted from neutron diffraction; Comparison of the experimental curve (dots) with the function backtransformed from the 2 Gaussian curves of the P-O peak model (solid line) using the parameters in Table 1.

Table 1. Coordination parameters obtained for the KPO_3 glass studied. fwhm stands for the full width at half maximum. Distances and fwhm are given in pm.

Atom pair	Coordination number	Distance	fwhm	Total coordination number	Mean distance
P-O	1.90 (5)	148.0 (10)	8.4 (10)	3.75 (10)	155 (1)
	1.85 (5)	162.5 (10)	10.7 (15)		
K-O	3.0 (5)	262.5 (20)	25 (2)	6.7 (5)	277 (2)
	3.7 (7)	288.5 (30)	25 (4)		
O-O	3.8 (2)	251.5 (15)	20 (2)		
P-P	2.0*	295.0*	25*	* fixed parameters	

corresponds to a distance difference of 14.3 pm. Hence, the two P-O bond lengths are confirmed by this rough estimation of the oscillation periods apparently dominating the neutron scattering curve.

All of the other pair distance peaks were superimposed with further ones. A combination of neutron and X-ray data is advantageous for their analysis. Different ratios of the weighting factors for the various pairs of atoms help to assign the contributions of the peaks in the total $T(r)$ functions shown in Figure 2. The large peak at 0.255 nm, attributable to O-O correlations belonging to the edges of PO_4 units, appears well pronounced in the neutron curve (Fig. 2a), while

its height is diminished in the X-ray curve (Fig. 2b). Thus, the contrast allows a reliable differentiation of O-O and K-O contributions, which are both expected in this distance interval.

The P-P distance corresponding to the P atoms of 2 tetrahedra linked with each PO_4 unit should amount 0.29 nm. A coordination number $N_{\text{PP}} = 2$ reflects the chain structure which is well confirmed by the ^{31}P magic angle spinning NMR [12] for metaphosphate glasses. Only a part of the observed peak at 0.29 nm in the X-ray $T(r)$ function (Fig. 2b) can be attributed to these P-P correlations. The main contribution of other correlations must belong to K-O contacts, while the shortest possible inter-tetrahedral P-O and O-O distances can only play a minor role. Otherwise, due to the enormous weight of P-O and O-O correlations in the neutron scattering, the corresponding $T(r)$ function would appear remarkably higher in this interval (Figure 2a). However, the P-P and K-O contributions can be poorly differentiated by use of the contrast of X-ray and neutron scattering. Hence, the values r_{PP} and N_{PP} were fixed during the fit (parameters see Table 1) while any P-O and O-O distances up to about 0.30 nm were neglected with the exception of the two peaks of intra-tetrahedral correlations with the parameters given in Table 1.

The most noticeable result is the peculiar shape of the K-O peak, which is approximated by a double maximum rather than by a broad single distance peak. Thereby it cannot be decided whether the K-O correlation diminishes to zero beyond this peak or continues with further K-O distances.

For distances exceeding 0.30 nm the structural information cannot be extracted simply as a superposition of peaks from contributions of all of the 6 possible pairs of atoms. An alternative analysis is found in the use of structural modelling. A suitable tool for combining experimental results from various methods is the Reverse Monte Carlo (RMC) simulation [13]. Continuous pair correlation functions can be derived from the mutual positions of atoms in a section of a possible 3-D glass structure generated by the simulations. Here only some RMC results concerning the short-range order will be shown.

The constraints for the atomic configurations in the RMC procedure were the neutron and the X-ray structure factors, informations about hard-core radii, and the knowledge about the P-O and O-P coordination numbers. The maximum of the N_{PO} value was 4, while only 2 of the 4 oxygen atoms in the PO_4 unit

were allowed to have 2 phosphorous neighbours. Thus, chains or rings form PO_4 tetrahedra were expected to be formed with the K^+ modifier cations embedded in large oxygen polyhedra.

The high- Q range of the neutron structure factor, $S(Q)$, was not included in the RMC simulations. Thus, the 2 different P-O bonds obtained by the least-squares fits cannot be reflected in the RMC results. It makes no sense to study the different bond lengths of bridging (BO) and non-bridging (NBO) oxygen atoms by RMC because no intrinsic correlation of the different oxygen sites with the unlike P-O bond distances exists in any of the experimental data exploited in the simulations. In case of the direct Monte Carlo method the interaction potentials contribute to the unlike P-O bonds in the PO_4 units where screening effects of charges play an eminent role.

Figure 4 shows a comparison of the model curve with the experimental X-ray $T(r)$ function. The broad P-O peak from the RMC simulations plotted in Fig. 4 reveals no useful information about the unlike P-O bonds. The partial correlations of the total X-ray $T(r)$ function (Fig. 4, lower part) show small contributions from P-O and O-O distances in the interval of the K-O peak. The small P-O peak at 0.26 nm and the sharp O-O peak at 0.22 nm were assumed to be artefacts from the simulations. However, minor contribu-

tions of these pair correlations being neglected in the least-squares fits cannot be excluded in the range of the right component of the first neighbour K-O peak. But there is no doubt, the typical shape of a double maximum of the K-O distances was confirmed by the RMC results.

4. Discussion

4.1 P-O Bond Lengths

Suzuki and Ueno [1] were the first to study an oxide glass by diffraction methods, whereby different types of oxygen bonds within the basic structural unit became evident. The double bond character of the P-NBO bond in the PO_4 tetrahedron of the NaPO_3 glass studied was concluded to be the reason for the remarkably shorter P-NBO distance compared with the P-BO bond length. Note, the different Ge-O bonds in alkali germanate glasses found by Ueno *et al.* [14] are caused by the existence of various GeO_n units.

Our first diffraction study using high real-space resolution [2] was performed on metaphosphate glasses with network modifier ions of medium and high electric field strength. It was found that not only the breadths of the P-O peaks depend on the field strength of the modifier cations, but also the distances themselves are influenced. The KPO_3 glass containing the large K^+ cations should show P-O bonds affected least by the modifier cations. The bond length difference of 14.5 pm is slightly larger than that found by Suzuki and Ueno [1] in a NaPO_3 glass (14.0 pm). But in [1] the distances were determined directly from the positions of the peak maxima. Therefore, only the distances from [2] will be taken for the comparison with the results obtained in this work. Figure 5 shows the P-O peaks of metaphosphate glasses. The frequencies of the unlike oxygen sites are equal in all of the 3 cases. Table 2 contains the P-O distances and the corresponding fwhm for the glasses. All of the changes are attributable to the influence of the different modifier cations with growing electric field strength in the order from K^+ to Al^{3+} . The fwhm of both P-O bond distributions are slightly increased in the same order, which indicates considerable distortions of the tetrahedra caused by the stronger Me-O interactions.

The changes of the P-O distances were explained by Gutmann's rules [3] about bond lengths under the influence of more or less strong atomic interactions in

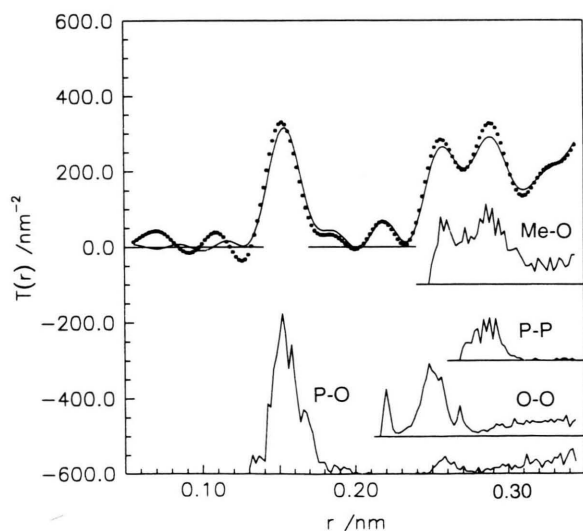


Fig. 4. Comparison of the experimental X-ray $T(r)$ function (dots) with that resulting from RMC simulations (solid line). The partial contributions in their original form are shown, shifted for clearness, in the lower part of the plot.

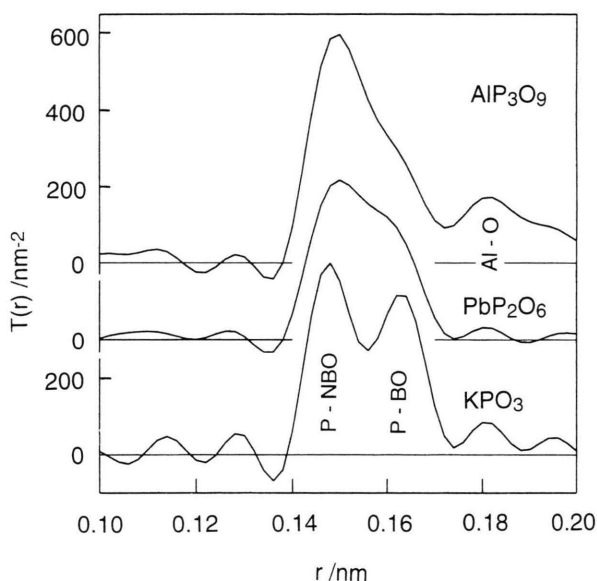


Fig. 5. Comparison of the P-O peaks in the neutron $T(r)$ functions of 3 metaphosphate glasses. The upper limit, Q_{\max} , chosen for the Fourier transformation, amounts to 420 nm^{-1} .

Table 2. P-O distances and full widths at half maximum (fwhm) for several metaphosphate glasses (K^+ : this work; the other values were taken from [2]); all of the values are given in pm.

Modifier cation	P-O distances			fwhm	
	mean	P-NBO	P-BO	P-NBO	P-BO
K^+	155.2	148.0	162.5	8.4	10.7
Pb^{2+}	154.5	148.5	160.5	10.0	12.0
$\text{Mg}^{2+}, \text{Zn}^{2+}$	154.3	148.0	160.0	10.0	13.4
Al^{3+}	154.0	149.1	159.1	11.1	16.7

their neighbourhood and are illustrated in Fig. 7 of [2]. The deformation of the electron population by these interactions elongates the P-NBO bond in case of a shift of the electron density from the positively charged P to the more negatively charged O atom of this bond pair, while the P-BO bond is shortened because of the resulting shift of the electrons, here oppositely from O to P. Due to the small electric field strength of the K^+ cation, the P-NBO bonds are the shortest while the P-BO bonds are the longest in the KPO_3 glass (Table 2). However, the rule about the elongation of the P-NBO bonds in the neighbourhood of very strong interactions with short distances between donor and acceptor [3] does not give an idea

about the effect by more or less covalent Me-O interactions. Quantitative predictions about the different influence of highly polarizable Pb^{2+} cations and Mg^{2+} cations on the length of an adjacent P-NBO bond are not simply possible. An estimation about the bond strength which is not only based on the Me-O distance and the nominal charge of the modifier cation, would be necessary.

The BO's and NBO's develop their specific character in the P-O bonds, which are additionally affected by the influence of various modifier cations. The diminished bond difference caused by stronger Me-O interactions results in more symmetric PO_4 tetrahedra. This effect is also indicated by the change of the isotropic chemical shift of the ^{31}P NMR line [12]. Moreover, the enlargement of the breadth to this NMR line with increasing modifier field strength [12] correlates with the increase of the fwhm values of the P-O distances (Table 2). Note, fully symmetrized PO_4 tetrahedra in which all P-O bonds are 156 pm are found in orthophosphates like AlPO_4 crystals [15]. The enlargement of the Me-O bond strength is attended by a slight diminishing of the mean of both P-O bond lengths (Table 2). This effect can be attributed to an overall strengthening of the glass network.

The changes of the P-O bonds in PO_4 middle groups under the influence of various alkali cations were studied by Uchino and Ogata using MO calculations [4]. The obtained tendencies harmonize with our experimental findings. The P-O distances in the $\text{K}_2\text{P}_2\text{O}_7$ model cluster, $r_{\text{P-NBO}}$ and $r_{\text{P-BO}}$, found to be 146.8 pm and 162.3 pm, respectively, well agree with our data determined for the KPO_3 glass. However, the MO calculations indicate a slightly different behaviour of the 2 NBO's in the PO_4 unit, resulting from an asymmetric position of the K^+ cation in respect of both NBO's with the P-NBO distances of 146.2 pm and 147.3 pm formed (see Fig. 6 bottom). Such distances cannot be differentiated by diffraction methods. Moreover, the width of the P-NBO peak shown in Fig. 2 is even smaller than that of the P-BO peak. Different from the $\text{K}_2\text{P}_2\text{O}_7$ cluster, in a glass structure every NBO atom is expected to have 2 or more K^+ neighbours, as plotted in Fig. 6 for a KPO_3 polyphosphate crystal (low temperature form) [6]. Thus, the conclusions drawn in [4] concerning the existence of 2 unlike NBO's, i.e. a predominantly double-bonded NBO and a more negatively charged one, should not be applicable to the KPO_3 glass.

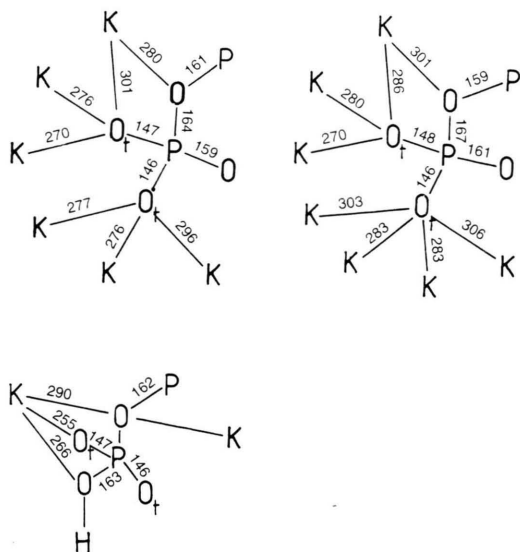


Fig. 6. K-O distances around the PO_4 tetrahedron; on top: Bond lengths around the 2 independent P positions in the polyphosphate crystal (low temperature form) [6]. Bottom: bond lengths around one of the 2 symmetric P positions from an ab initio MO calculation [4]. O_t is the terminal oxygen.

4.2 K-O Coordination Sphere

The K-O distance peak on the KPO_3 glass (Fig. 2) is splitted into 2 components located at distances, r_{KO} , of 262 pm and 288 pm. Both components yield equal contributions to the total coordination number, N_{KO} , of about 6.7. In a former study on a sodium disilicate glass and a sodium metaphosphate glass [5] the Na-O peak was found to be splitted for the silicate environment but not splitted for the phosphate system. Note, in the disilicate system the number of NBO's per Na^+ cation is only half of that present in the metaphosphate glass. In the related crystals of the disilicate system and the KPO_3 glass, respectively, the BO's are found to be involved in the environment of the modifier cations, but this fact is not observed in the sodium phosphate crystals. In Table 3 the N_{KO} and r_{KO} values of the K-O distance peaks, which are splitted for most of the crystals, are compared with the corresponding values for the glass. For illustration of the similarity to the behaviour of the Na^+ cations in the silicate environment, the corresponding parameters of the disilicate glass and the related crystals are given. Note, in the KPO_3 glass and in the sodium disilicate glass the N_{MeO} and r_{MeO} values appear slightly smaller than in the related crystals.

The breakage of links between the tetrahedral units accompanied by the formation of non-bridging oxygens caused by modifier oxide additions is a common characteristic of silicate and phosphate glasses. The cations are accommodated close to the negatively charged non-bridging oxygens so as to maintain local electroneutrality in the structure [21]. In general, the NBO atoms have more than one modifier cation as neighbour aimed at improving the charge compensation. It was shown [4, 22] that the other oxygen atoms in the glass structure are negatively charged, as well. Hence, for ultraphosphate glasses with their large amount of terminal oxygen atoms it was concluded [23] that the double-bonded oxygen atoms of the branching groups tend to coordinate a modifier cation which was found to be relevant for the explanation of observed Me-O coordination numbers. The BO's occupying positions screened between 2 positively charged P atoms show little tendency to coordinate a modifier cation. Uchino and Ogata have shown [4] that, contrary to the behaviour of the Na^+ , the K^+ cations prefer positions with great numbers of adjacent oxygens atoms, i.e. NBO's and even BO's. The large radius of the K^+ prevents a compensation of its positiv charge over a short distance. However, the screening effect of the P atoms does not hinder the BO's to be incorporated in the K^+ cations coordination sphere at the large K-O distances.

Table 3. Me-O distances and Me-O coordination numbers for the potassium metaphosphate glass (KPO_3) studied and a sodium disilicate glass ($\text{NaSiO}_{5/2}$) [5] compared with the values of related crystals. The distances are given in pm.

Structure	Me-O coordination number		Me-O distance		Reference
	N_1	N_2	r_1	r_2	
KPO_3 glass	3.0	3.7	263	288	this work
T-polyphosphate*	5.0	2.5	278	302	[6]
Z-polyphosphate*	5.0	2.0	283	320	[6]
H-polyphosphate*	8.0		303		[16]
3-cyclophosphate	4.0	1.0	275	314	[17]
6-cyclophosphate	5.0	1.0	276	319	[18]
$\text{NaSiO}_{5/2}$ glass	2.5	2.5	225	253	[5]
α -phyllosilicate	4.0	1.0	235	260	[19]
β -phyllosilicate	3.5	2.0	239	253	[20]

* T, Z, and H mean the low-, medium, and high-temperature modification of the potassium polyphosphate crystal, respectively.

From the reference to the sodium disilicate glass [5], we deduce the deficit of oxygen atoms to be the essential reason for the BO's involvement in the K-O spheres. But this fact does not explain that the K-O peak is obtained to be splitted. At first sight it appears meaningful to suppose the BO's to be related to the second peak component. However, in all of the crystal data listed in Table 3 the Me-BO distances are found in both peak components, which is illustrated in Fig. 6 top. The MO calculations [4] reveal a short and a long K-BO distance (Fig. 6 bottom). Thus, a definite relation of the formation of 2 well pronounced K-O distances to the behaviour of the BO's is not evident, but a correlation between both phenomena should exist.

We suggest the following: Most of the NBO are attached to 3 K^+ cations. These modifier ions located in the vicinity of a given NBO must be positioned on corners of a equilateral triangle in order to form a single K-O distance peak. This arrangement does not lead to a stable equilibrium of the interaction forces because of 2 facts: The strong P-O bonds permit little flexibility of the positions of NBO's. Furthermore, the K^+ cations concurrently have to find a suitable position against 6 or more oxygen atoms. From an energetical point of view it is most favourable for the modifier cation to contact 3 oxygen atoms. The weak K-O interactions cannot form KO_n polyhedra with K-O distances being nearly equal. An adequate explanation was given [5] for the Na^+ cation in a disilicate glass. The asymmetry of the polyhedra is also observed in the KPO_3 crystal which is illustrated in Fig. 6 top.

5. Conclusions

The existence of 2 P-O bond distances has confirmed the assumption that oxygen atoms in the PO_4 middle group must be divided into the bridging and the terminal (non-bridging) ones. There is no indication for a further differentiation of the terminal positions. A comparison with former results of glasses containing modifier cations of high electric field strength corroborates the conception about the P-O bond lengths being changed under the influence of the modifier ions. In presence of the K^+ cation, the splitting of the P-O peak is largest and the widths of both peak components are smallest.

The K-O coordination sphere shows 2 pronounced K-O distances. This effect is similar to the behaviour of oxygen positions around a Na^+ cation in a disilicate glass. Taking into account the structures of related crystals and the results of ab initio MO calculations, the participation of the BO's in the K-O coordination is most likely, but their function in this process remains unclear. The competition of the K^+ cations for the oxygen atoms can explain the K-O peak shape. In this process the presence of weak K-O interactions besides strong P-O bonds is responsible for the formation of very asymmetric KO_n polyhedra.

Acknowledgements

The financial support of the Deutsche Forschungsgemeinschaft (grand WA 842/1-2) is gratefully acknowledged.

- [1] K. Suzuki and M. Ueno, *J. de Physique* **46**, C8-261 (1985).
- [2] U. Hoppe, G. Walter, D. Stachel, and A. C. Hannon, *Z. Naturforsch.* **50a**, 684 (1995).
- [3] V. Gutmann, in: *The Donor-Acceptor Approach to Molecular Interactions*, Plenum Press, New York 1978, pp. 4-16.
- [4] T. Uchino and Y. Ogata, *J. Non-Cryst. Solids* **191**, 56 (1995).
- [5] U. Hoppe, D. Stachel, and D. Beyer, *Physica Scripta* **T57**, 122 (1995).
- [6] K. H. Jost and H. J. Schulze, *Acta Crystallogr.* **B25**, 1110 (1969).
- [7] A. C. Hannon, W. S. Howells, and A. K. Soper, in: *Proceedings of the Second Workshop on Neutron Scattering Data Analysis*, ed. M. J. Johnson, IOP Conf. Series **107**, Chilton 1990, pp. 193-211.
- [8] U. Hoppe, G. Walter, and D. Stachel, *Phys. Chem. Glasses* **33**, 216 (1992).
- [9] T. E. Faber and J. M. Ziman, *Phil. Mag.* **11**, 153 (1965).
- [10] Y. Waseda, in: *The Structure of Non-Crystalline Materials*, McGraw-Hill, New York 1980, p. 11 ff.
- [11] A. J. Leadbetter and A. C. Wright, *J. Non-Cryst. Solids* **7**, 23 (1972).
- [12] R. K. Brow, C. C. Phifer, G. L. Turner, and R. J. Kirkpatrick, *J. Amer. Ceram. Soc.* **76**, 1287 (1991).
- [13] R. L. McGreevy and L. Pusztai, *Mol. Simulation* **1**, 359 (1988).
- [14] M. Ueno, M. Misawa, and K. Suzuki, *Physica* **120B**, 347 (1983).
- [15] R. C. L. Mooney, *Acta Crystallogr.* **9**, 728 (1956).
- [16] K. H. Jost and H. J. Schulze, *Acta Crystallogr.* **B27**, 1345 (1971).
- [17] M. Bagieu-Beucher, I. Tordjman, A. Durif, and J. C. Guitel, *Acta Crystallogr.* **B32**, 1427 (1976).
- [18] M. T. Averbuch-Pouchot, *Acta Crystallogr.* **C45**, 1273 (1989).
- [19] A. K. Pant and D. W. J. Cruickshank, *Acta Crystallogr.* **B24**, 13 (1968).
- [20] A. K. Pant, *Acta Crystallogr.* **B24**, 1077 (1968).
- [21] H. Rawson, in: *Materials Science and Technology. A Comprehensive Treatment*, Vol. 9, ed. J. Zarzycki, VCH, Weinheim 1991, pp. 281.
- [22] T. Uchino and Y. Ogata, *J. Non-Cryst. Solids* **181**, 175 (1995).
- [23] U. Hoppe, *J. Non-Cryst. Solids*, in press.